Spin Resonances of F_2^- Ions and Hydrogen Atoms in Electron-Irradiated Ammonium Bifluoride and Sodium Bifluoride*

LAWRENCE J. VANDE KIEFT† AND O. R. GILLIAM
Department of Physics and Institute of Materials Science, University of Connecticut, Storrs, Connecticut 06268

(Received 3 October 1969)

Radiation effects in single crystals of ammonium bifluoride and sodium bifluoride were studied by electron spin resonance (ESR) and optical methods following 1-MeV electron irradiations at 77°K. The irradiations changed the samples from clear to deep blue-green, and both crystal types showed paramagnetic resonances which were determined to result from F_2^- ions in anion sites. This defect resulted from the displacement of hydrogen atoms from their normal positions in the linear bifluoride $(FHF)^-$ ions. Only in NH_4HF_2 were the displaced hydrogen atoms detected. Best-fit spin-Hamiltonian parameters for the F_2^- and H^0 defects are given. Optical-absorption measurements on the irradiated bifluorides are discussed. The ESR annealing characteristics for the F_2^- ions in both crystals appear to follow second-order kinetics. In two of the three inequivalent sites for F_2^- ions in NH_4HF_2, the orientation of the F_2^- molecular axis differs by 8° from the reported crystallographic axis of the corresponding bifluoride anion. This is interpreted to result from weaker hydrogen bonding between nitrogen and fluorine for the F_2^- ion than for the bifluoride ion in ammonium bifluoride, because of an increased N—H—F distance for the shorter F_2^- ions.

I. INTRODUCTION

ELECTRON-SPIN-RESONANCE (ESR) measurements have been conducted to study radiation effects in single crystals of ammonium bifluoride (NH_4HF_2) and sodium bifluoride ($NaHF_2$). Earlier work on radiation effects in bifluorides has consisted of the study by ESR and optical-absorption techniques of F_2^- ions trapped in potassium bifluoride (KHF_2) following electron bombardment at 77°K.[1] In that investigation the KHF_2 crystals were found to be highly resistant to radiation damage by Co^{60} γ-ray irradiation, but susceptible to damage by electron irradiation for electron energies as low as 0.15 MeV. It was presumed that the F_2^- ion was formed via the displacement of the hydrogen atom to an interstitial site, however, evidence of the trapped hydrogen atom was not found. Similar investigations have now been made on NH_4HF_2 and $NaHF_2$. All three types of bifluoride crystals have in common the same anion radical, the linear $(FHF)^-$ ion. However, they have different crystal symmetries and would be expected to yield different results upon irradiation. In contrast to potassium bifluoride, which is body-centered tetragonal in structure, the ammonium bifluoride crystal lattice is orthorhombic, and the sodium bifluoride lattice is rhombohedral. It was expected that electron irradiations might make possible a comparative study of F_2^- ions in these dissimilar crystal lattices. Moreover, it was recognized that trapped hydrogen atoms, if detected following irradiation, would further substantiate the radiation damage process suggested previously for the irradiated KHF_2.

II. CRYSTAL STRUCTURES

A. Ammonium Bifluoride

The orthorhombic ammonium bifluoride crystal structure is shown in projection in Fig. 1. This crystal corresponds to the space group $V_h^7(Pman)$; its tetramolecular unit has the following lattice parameters: $a_0=8.408$ Å, $b_0=8.163$ Å, and $c_0=3.670$ Å.[2] The structure is rather unique in that it is determined completely by hydrogen bonds. In KHF_2, each potassium ion has eight equidistant fluorine neighbors, while in NH_4HF_2 four of the eight fluorine ions surrounding the nitrogen

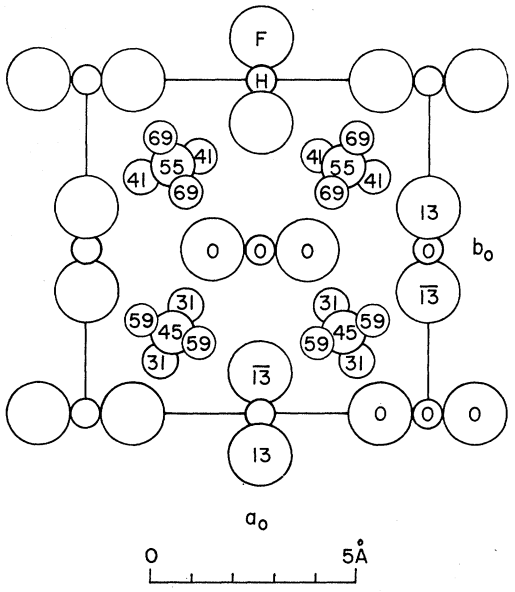

FIG. 1. Projection of the orthorhombic structure of NH_4HF_2 along its c_0 axis (from Ref. 2).

* Research supported by the U. S. Atomic Energy Commission.

† Present address: U. S. Army, Aberdeen Research and Development Command, Aberdeen Proving Ground, Md.

[1] Fred B. Otto and O. R. Gilliam, Phys. Rev. **154**, 244 (1967).

[2] R. W. G. Wyckoff, *Crystal Structures* (Interscience Publishers, Inc., New York, 1964), Vol. 2, Chap. 6.

atom tetrahedrally are contracted to the distance 2.82 ± 0.02 Å through the formation of N–H–F hydrogen bonds, the other four being at about 3.1 Å.[3] The $(FHF)^-$ ions in NH_4HF_2 exist in three inequivalent sites. The ions with their major symmetry axes along the a_0 axis are designated as residing in the site $S(1)$. Those in the two sites designated $S(2)$ lie in the b_0c_0 plane. In a perfect crystal neglecting boundary effects, there are the same number of $S(2)$ sites as of $S(1)$ sites, but the $S(2)$ sites are equally divided into those tilted up and those tilted down relative to the a_0b_0 plane. This tilt angle is $\pm21.4°$. The $(FHF)^-$ ions in the $S(1)$ and $S(2)$ sites have almost identical fluorine-fluorine distances[2]:

$$S(1) \quad F\text{–}H\text{–}F = 2.275 \text{ Å},$$
$$S(2) \quad F\text{–}H\text{–}F = 2.269 \text{ Å}.$$

B. Sodium Bifluoride

Sodium bifluoride forms rhombohedral crystals with the following lattice parameters[2]:

$$a_0=b_0=c_0=5.004 \text{ Å} \quad \text{and} \quad \alpha=40°\,33',$$

for the rhombohedral unit cell which is pictured in Fig. 2. This crystal structure can also be described in terms of a hexagonal unit cell. If the latter description is used, the parameters are: $a_0=b_0=3.468$ Å and $c_0=13.76$ Å (at 25°C).[2]

III. EXPERIMENTAL PROCEDURES

The crystals required for this investigation were grown from saturated aqueous solutions using a closed system whose temperature was programmed to decrease very slowly. Good optical-quality crystals of NH_4HF_2 were obtained; the $NaHF_2$ crystals were of good quality but were small enough to cause difficulty in handling, orientation, and optical-absorption measurements. Samples were oriented by use of a polarizing microscope, x-ray backscatter photographs, and x-ray precession photographs. All the principal translation vectors were determined relative to the facets and edges of the crystals. NH_4HF_2 crystals were shaped by grinding flats perpendicular to the crystallographic axes. This facilitated mounting them in microwave resonant cavities and in the Cary-14R spectrophotometer. The $NaHF_2$ crystals were too small to grind easily so a special TE_{102} rectangular cavity was built having a rotatable sample pedestal in a narrow side of the cavity. The sample pedestal had an axis of rotation which was perpendicular to the axis about which the dc magnetic field could be made to rotate. These two degrees of freedom made it possible to obtain any orientation of the crystal relative to the magnetic field for ESR angular-variation measurements.

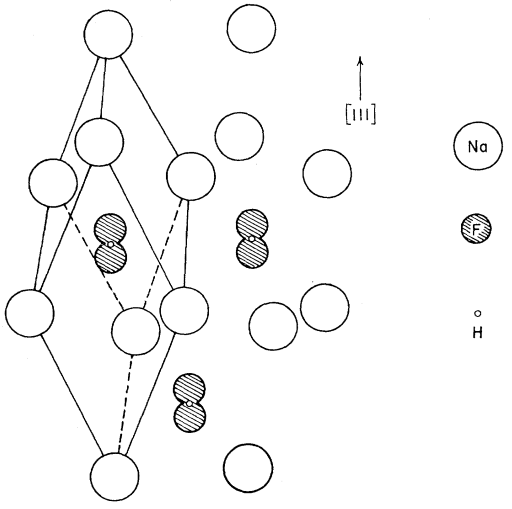

FIG. 2. Portion of the $NaHF_2$ structure showing three $(FHF)^-$ ions. The rhombohedral unit cell is outlined.

The NH_4HF_2 and $NaHF_2$ samples were subjected to ionizing radiation of two types, γ rays and high-energy electrons. The γ rays were supplied by a Co^{60} γ-ray source and the electrons by a 1-MeV Van de Graaff accelerator. Electron irradiations were made at about 1-MeV energy and 1-μA beam current for periods from 5 min to 1 h. Background ESR runs and optical absorption runs were made prior to irradiation. After irradiation, ESR data were taken at about 9.2 GHz with a superheterodyne spectrometer having usable power levels up to 12 mW, and optical-absorption measurements were made using the Cary-14R spectrophotometer. Both bifluoride crystals were investigated using unpolarized light to determine which absorption bands were produced by the radiation. Then further optical-absorption spectra were obtained, this time using polarized light. Background runs had been made for each polarization, and the effectiveness of the polarizers had been measured. The transmission ratio for the polarizers, crossed to parallel, was less than 1%.

Pulse annealing studies of the spin resonances were made to determine activation energies of the radiation-induced defects using a variable temperature microwave cavity. This was a TE_{102} rectangular cavity modified for operation from 77°K to above room temperature.[4] A thermocouple was mounted on the cavity near the sample location and a heating element was mounted just above the cavity. A length of stainless-steel waveguide was connected just above the heater, for thermal isolation, and this system was enclosed in a brass cylinder. In operation, the cylinder was immersed in liquid nitrogen. For heating, the cylinder was evacuated of gas and electrical power was supplied to the heating element. For cooling, power was removed and helium gas was admitted to the cylinder to thermally link the

[3] L. Pauling, *The Nature of the Chemical Bond* (Cornell University Press, Ithaca, N. Y., 1960), 3rd ed., p. 462.

[4] F. T. Gamble, R. H. Bartram, C. G. Young, O. R. Gilliam, and P. W. Levy, Phys. Rev. **138**, A577 (1965).

resonant cavity and sample to the liquid nitrogen. The thermocouple was used to monitor the sample temperature during the annealing experiment.

All resonance-line intensities were measured at 77°K in the pulse annealing studies to maintain the same spectrometer performance and the same Boltzmann factor for population of energy levels. The times required for temperature changes were short compared to the period of the annealing pulse; corrections for these shorter times could not be applied to the data.

IV. RESULTS

Samples of ammonium bifluoride and sodium bifluoride single crystals were exposed to 10^6R Co^{60} γ-ray irradiations at 300 and at 77°K and ESR runs were made without warmup from the irradiation temperature. No spin resonances were observed. However, irradiation at 77°K with about 10^{15} 1-MeV electrons changed the colorless crystals to a deep blue-green, and large paramagnetic resonances were recorded. In NH_4HF_2, most of the resonance lines were about 15 G broad but two lines were about 65 G wide corresponding to a different paramagnetic species. In $NaHF_2$, only the narrower type of resonances appeared.

A. Characteristics of ESR Spectra

Angular-variation measurements about three orthogonal axes in the irradiated crystals were performed to characterize the paramagnetic defects. These variations are shown for NH_4HF_2 in Figs. 3 and 4, in which dc

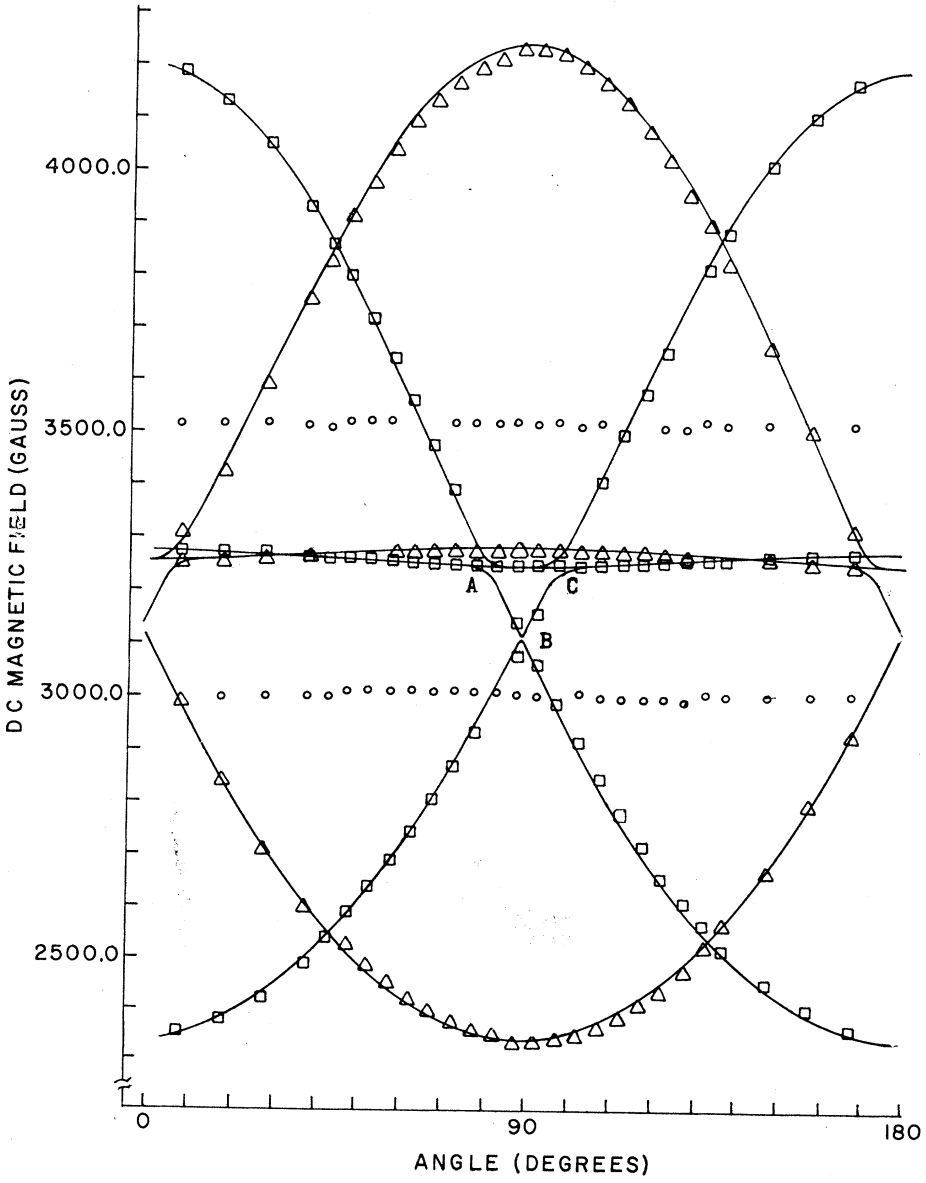

FIG. 3. Graph of the experimental resonance positions and computed curves (solid lines) for the c_0-axis angular variation for NH_4HF_2 after electron irradiation at 77°K. The squares represent resonances attributed to F_2^- ions in two inequivalent sites which give overlapping spectra for this angular variation; these sites are related to the sites of bifluoride ions which are tilted with respect to the a_0b_0 plane. The triangles represent data for an F_2^- defect in an untilted anion site. The circles give the magnetic field values for resonances of a defect identified as a neutral hydrogen atom. The microwave frequency was 9.151 GHz.

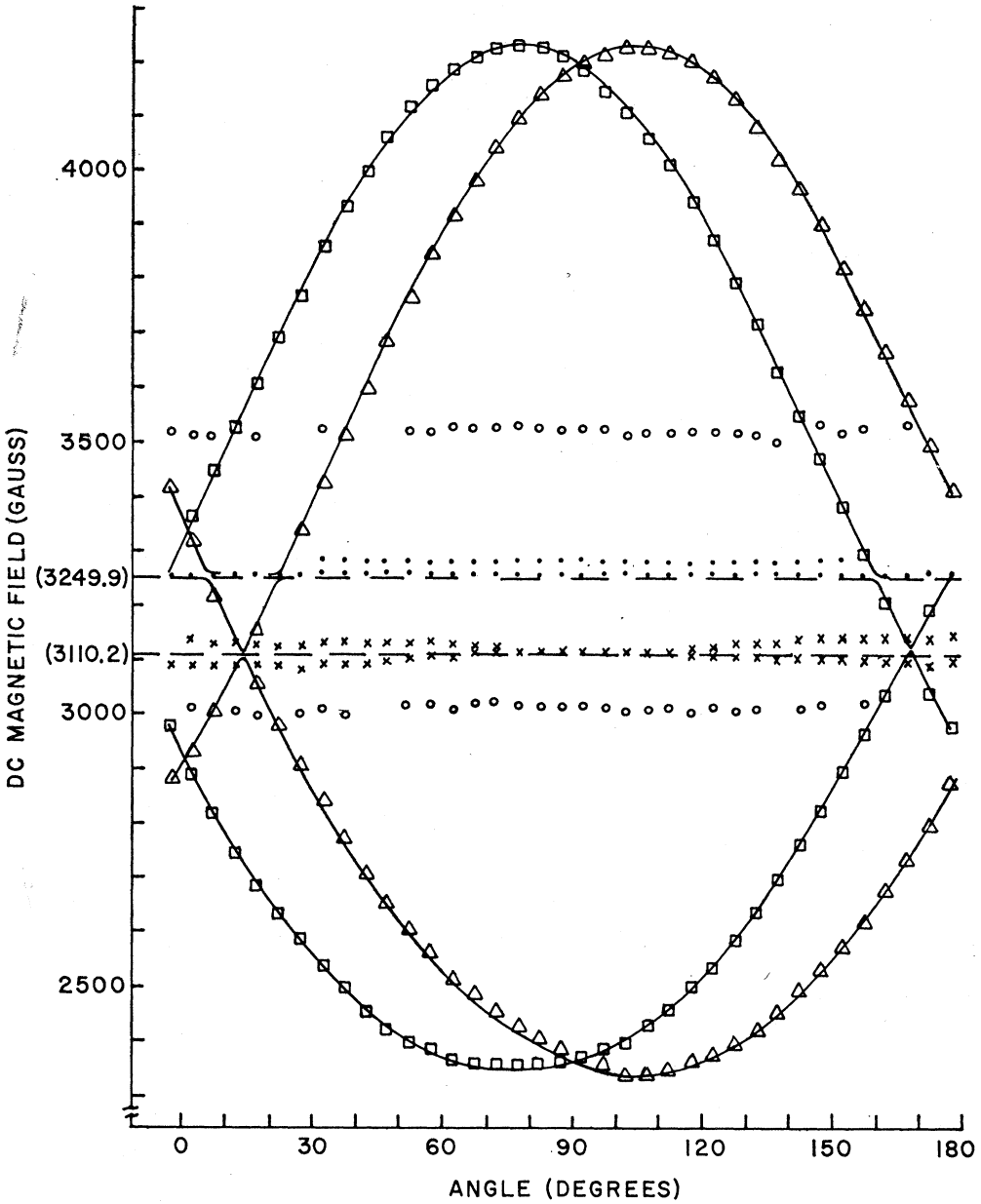

FIG. 4. Comparison of the experimental and computed resonance positions for the a_0-axis angular variation for NH_4HF_2 after electron irradiation at 77°K. The squares and triangles represent experimental points for F_2^- ions in the two inequivalent sites of anions which are tilted with respect to the a_0b_0 plane. One row of dots represents spectral lines associated with those designated by triangles, the other row of dots is part of the spectra designated by squares. The ×'s correspond to F_2^- ions in a third inequivalent anion site. The circles represent the data for trapped hydrogen atoms. The microwave frequency was 9.163 GHz.

magnetic field values for resonance are plotted as experimental points. The solid lines represent the theoretical angular variations predicted from best-fitting spin-Hamiltonian parameters. Figure 3 displays the c_0-axis angular variation; the independent variable corresponds to the angle between the b_0 axis and the magnetic field. Figure 4 represents a rotation about the a_0 axis, the angle plotted corresponding to that between the c_0 axis and the field. It was evident from the angular-variation plots, and from linewidths and annealing behaviors, that two defect species were generated by the bombardment. The circles in these figures represent data for an isotropic spin-$\frac{1}{2}$ defect with an isotropic two-line hyperfine structure. The resonances represented by triangles and squares can be attributed to a slightly anisotropic spin-$\frac{1}{2}$ defect (in three inequivalent sites) coupled with a highly anisotropic hyperfine interaction with two nuclei of spin $\frac{1}{2}$. Arguments are presented in Sec. V that these two defects are neutral hydrogen atoms and F_2^- ions, respectively.

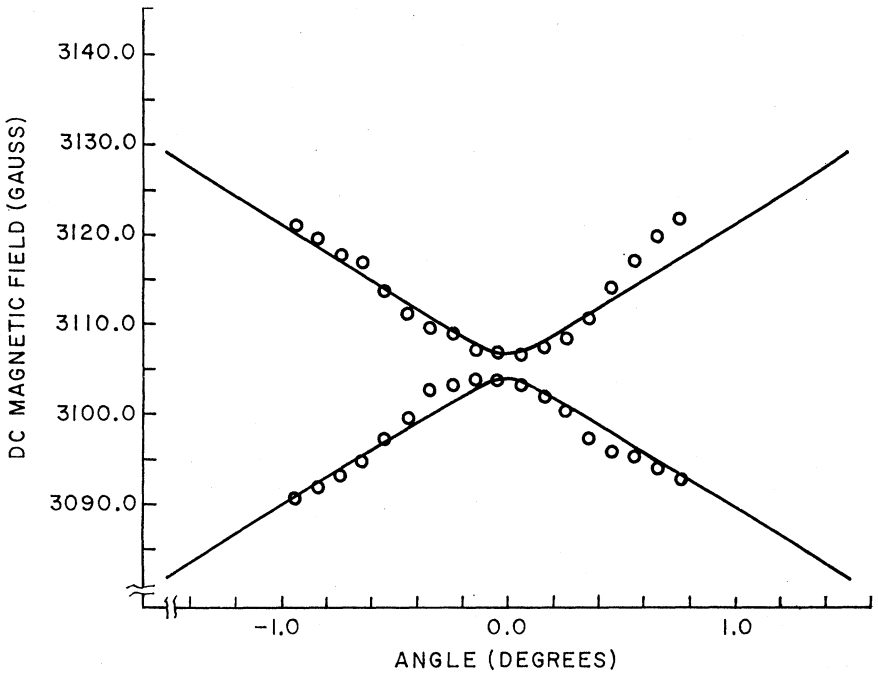

FIG. 5. Comparison of experimental and computed positions in a region of an apparent crossing of resonance lines for untilted F_2^- ions in a b_0-axis angular variation. This plot represents a detailed investigation of a region similar to region *B* in Fig. 3, which is for the tilted ions. The frequency was 9.178 GHz.

The resonances attributed to F_2^- ions are found in three inequivalent sites which are closely related to the anion sites in the unirradiated crystal. The major axis of symmetry for this paramagnetic defect corresponds to the orientation which gives maximum splitting of its set of resonance lines. For such an orientation the dc magnetic field is parallel to the (F–F) bond direction. For one of the inequivalent sites, this axis lies along the [100] direction, which is identical to the symmetry axis of a bifluoride ion in an $S(1)$ site (see Sec. II). For the other two inequivalent sites, the major axes make angles of $\pm 13.4°$ with respect to the [010] direction and lie in the b_0c_0 plane. These defect sites, although they appear related to the crystallographic anion sites $S(2)$, have shifted symmetry axes. For the anion sites $S(2)$ the angle that the bifluoride symmetry axis makes with the [010] direction according to x-ray structural analysis is reported as $\pm 21.4°$.[2] In further discussions the sites of the F_2^- defect are referred to as "untilted" and "tilted" sites and the related ESR absorptions as "untilted" and "tilted" lines, or as "untilts" and "tilts."

There are three positions shown in Fig. 3 in the spectrum of the F_2^- defects where the resonance lines appear to have an anomalous behavior. These points are labelled A, B, and C for the tilts. There would be similar points for the untilts near the 0° and 180° regions of the curves. These anomalous points for the tilts were investigated in detail at higher gain settings in the vicinity of 0° to see whether or not the lines crossed. The results for untilts are plotted in Fig. 5 where the individual points are experimentally determined and the solid lines are the theoretically generated predictions. It can be seen that the lines approach each other and then separate again without crossing. At the closest point of approach the lines were unresolved and the separation was determined by comparing the separation between inflection points of the combined absorption to the corresponding type of measurement for a single resolved line at a slightly different angle. The same behavior was observed for the tilted lines when investigated in detail near 90° in Fig. 3.

Radiation damage to potassium bifluoride has been previously investigated,[1] and the F_2^- defect was identified; but its complementary defect, the trapped H^0, was not found. Before beginning work on the sodium and ammonium bifluorides, the authors tried to find the H^0 defect in KHF_2 by electron irradiating near liquid-helium temperature and making ESR runs prior to warmup. Still, the H^0 defect was not found. However, in NH_4HF_2 the H^0 atoms were observed by ESR following electron irradiation at 77°K, having been displaced from their normal $(FHF)^-$ sites and trapped elsewhere in the crystal lattice. The two resonance lines in Fig. 3 which show no variation of the resonant magnetic field as a function of angle and whose experimental points are designated by circles are due to this defect. The separation between them, which is 513 ± 9 G, is a measure of the hyperfine coupling constant for a hydrogen atom in this site. The isotropic character of this electronic transition and of the two-line hyperfine structure contributes to the identification of the defect as H^0, but it furnishes no information about the character of the site.

In $NaHF_2$, the H^0 resonances were not detected for electron irradiation and observation at 77°K. However, an ESR spectrum was obtained for the F_2^- defect which

was similar to that recorded for each inequivalent site in irradiated NH_4HF_2. The F_2^- defect was found to reside in only one site in $NaHF_2$ and it possessed symmetry corresponding to that of the bifluoride anion.

B. Analysis

All observed ESR spectra could be fitted to a spin Hamiltonian of the form

$$\mathcal{H}=\beta_0\mathbf{H}\cdot\mathbf{g}\cdot\mathbf{S}+\mathbf{S}\cdot\mathbf{A}\cdot\mathbf{I}-g_N\beta_N\mathbf{H}\cdot\mathbf{I}.$$

For the F_2^- defect $S=\frac{1}{2}$, $I=I_1+I_2$, and $I_1=I_2=\frac{1}{2}$, while for the hydrogen neutral atoms, $S=\frac{1}{2}$ and $I=\frac{1}{2}$. The components of the g and A tensors were computed from the experimental data. For the H^0 defect the values of the spectroscopic splitting factor and of the hyperfine coupling constant are immediately obtained from the measurements, independent of crystal orientation. For the F_2^- defect, precision measurements were made of resonant magnetic field and microwave frequency for the crystal orientations which gave maximum and minimum splittings of the ESR spectral lines. However, the anisotropy in the A tensor is so large that the approximate equations given by Bleaney for determining the parameters are inadequate.[5] Instead the 8×8 spin-energy matrix was employed, as previously[1,6]; for the special orientations referred to above, this matrix reduces to a partitioned form with two 3×3 and one 2×2 submatrices. The matrix elements have the form $\langle i|H/g_0\beta_0|j\rangle$, where the wave functions are $|SM_S\rangle|IM_I\rangle$, with $S=\frac{1}{2}$ and $I=0$, 1. The partitioned matrix is easily diagonalized, and from the resulting relations $A_{\|}$, $g_{\|}$, and $g_\perp$ can be calculated. Using the values for these parameters, a digital computer was used to generate resonance field values for a given orientation as a function of $A_\perp$. Comparison of these results with experimental data gave the correct value for $A_\perp$. Four modifications of the basic computer program were used. In addition to computing $A_\perp$, angular variations were generated for both tilted and untilted ions, which are plotted as solid-line curves in Figs. 3 and 4. The determined spin-Hamiltonian parameters for F_2^- ions in NH_4HF_2 and in $NaHF_2$ and for H^0 in NH_4HF_2 are given in Table I.

C. Linewidths and Line Shapes

Determinations of linewidths and line shapes for the F_2^- defects and for the trapped H^0 atoms were made at 77°K. The linewidth for the F_2^- defect was found to vary with sample orientation. For the c_0-axis angular variation in NH_4HF_2 linewidths were measured at 88.2° near region B for the two resolved F_2^- lines. The line at the lowest field value measured 19.9 G between inflection points, and the adjacent resolved line measured 21.2 G. Measured widths of the untilted lines for an angle similarly near the point of closest approach of the resonances were 13.1 and 12.9 G. These linewidth measurements were used in a determination of the minimum value of separation of these resonances in the angular variation. For $NaHF_2$, the variation in linewidth with orientation was investigated in more detail. For defect polar angles of 0°, 35°, 70°, and 105°, the high-field F_2^- resonance line measured 10.1, 13.1, 14.3, and 13.3 G wide, respectively. There appeared to be a systematic variation of linewidth with angle, the narrowest being near $\theta=0°$ and the widest being at $\theta=90°$. No structure was detected on this resonance line at 77°K. The two lines resulting from the trapped hydrogen atoms in NH_4HF_2 were 65 G wide. This greater width accounted for their lower amplitude, which reduced measurement precision for the H^0 spin-Hamiltonian parameters. The shape of the H^0 lines was Gaussian and that of the F_2^- lines appeared to be a mixture of Gaussian and Lorentzian. In $NaHF_2$, the F_2^- resonances were Gaussian.

D. Annealing Results

Pulse annealing experiments were done on the F_2^- defects in both the ammonium and sodium bifluoride crystals. If the annealing obeyed the equation for first order kinetics, namely $dN/dt=-KN$, where N is the concentration of defects, K is the rate constant and t is the time, then a plot of log N versus t would be a straight line for a given temperature. If second-order kinetics were followed, then $dN/dt=-KN^2$ and a plot of $1/N$ versus t would be a straight line for constant K. The latter type of plot of the experimental results is shown in Fig. 6. It is apparent that the plots for three annealing temperatures approximate straight lines indicating second-order kinetics. The fit to first-order kinetics (not shown) is poor. Each ESR measurement of line intensity was made at 77°K. The small curvature of the locus of data points might result from the lack of corrections for the times required for temperature changes in the pulse annealing experiments, or from an appreciable concentration dependence of K for the second-order equation. The decay of F_2^- ions in $NaHF_2$ is also found to be a second-order process; for rates of decay similar to those measured in NH_4HF_2, the required annealing temperature is about 30 deg higher. If one assumes that K equals a constant times the Boltzmann factor $e^{-E/kT}$, an activation energy E can be computed.[7] Values calculated are approximately 0.14 and 0.4 eV in NH_4HF_2 and $NaHF_2$, respectively. Insufficient data were obtained to compare the H^0 annealing characteristics with those of the F_2^- in NH_4HF_2; the unannealed amplitude of the H^0 resonance was small because of the large linewidth.

E. Optical Measurements

The measured optical spectra of the two bifluoride crystals are similar. Only one prominent absorption

[5] B. Bleaney, Phil. Mag. **42**, 441 (1951).
[6] T. O. Woodruff and W. Kanzig, J. Phys. Chem. Solids **5**, 268 (1958).
[7] A. W. Overhauser, Phys. Rev. **90**, 393 (1953).

TABLE I. Measured spin-Hamiltonian parameters for radiation-induced defects in electron-irradiated NH_4HF_2 and $NaHF_2$ at 77°K.

	g_z	g_x	g_y	A_z (in G)	A_x (in G)	A_y (in G)
F_2^- in NH_4HF_2	1.9998 ±0.0003	2.0152 ±0.001	2.0152 ±0.001	948.1 ±0.3	15.9 ±0.1	20.6 ±0.1
F_2^- in $NaHF_2$	2.0001 ±0.0003	2.0158 ±0.001	2.0158 ±0.001	984.6 ±0.3	64.0 ±0.1	64.0 ±0.1
H^0 in NH_4HF_2	$g_z=g_x=g_y=2.006\pm0.004$			$A_z=A_x=A_y=513\pm9$ G		

band was observed for each of the crystals; it is shown in Fig. 7 for NH_4HF_2. The center of this band was in the ultraviolet at 306 mμ for NH_4HF_2 and at 308 mμ for $NaHF_2$. This particular absorption band by its annealing behavior and dichroic character appeared to be correlated with the F_2^- defect in the respective crystals.

Delbecq, Hayes, and Yuster[8] report two optical absorption bands correlated with the V_K center in LiF; this F_2^- defect in LiF gives a strong absorption band at 348 mμ and a barely detectable band at 750 mμ. The strong band is described as completely anisotropic with transitions allowed only for light with the electric vector parallel to the molecular axis of the F_2^- ions. Thus the transition is described as σ-polarized. Both observed transitions have been explained[8] by a molecular orbital energy level scheme[9,10] consisting of a single σ_g orbital, two π_u orbitals, two π_g orbitals, and a single σ_u orbital in order of increasing energy. All of these orbitals are filled except for the σ_u orbital which has only a single

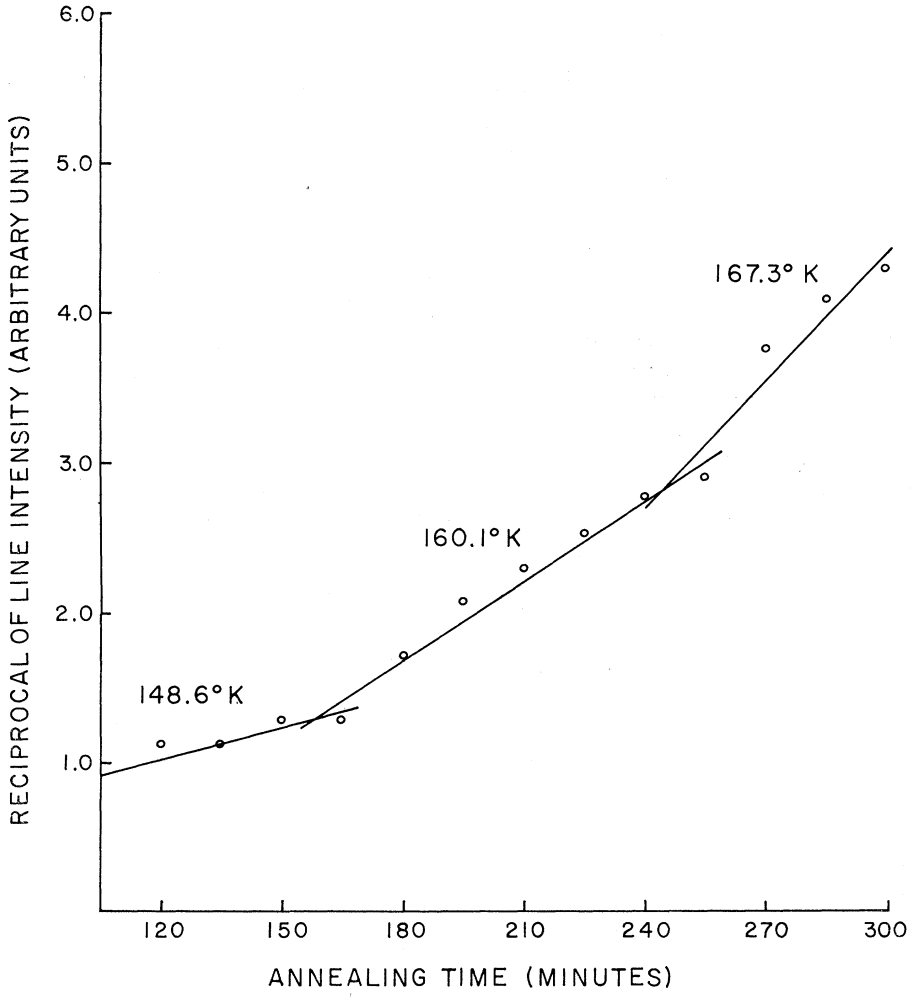

FIG. 6. Validation of second-order kinetics as a description of the annealing process for F_2^- ions in electron-irradiated NH_4HF_2. Pulse anneals were employed with the line intensity measurements at 77°K.

[8] C. J. Delbecq, W. Hayes, and P. H. Yuster, Phys. Rev. **121**, 1043 (1961).
[9] M. H. Cohen, Phys. Rev. **101**, 1432 (1956).
[10] T. Inui, S. Harasawa, and Y. Obata, J. Phys. Soc. Japan **11**, 612 (1956).

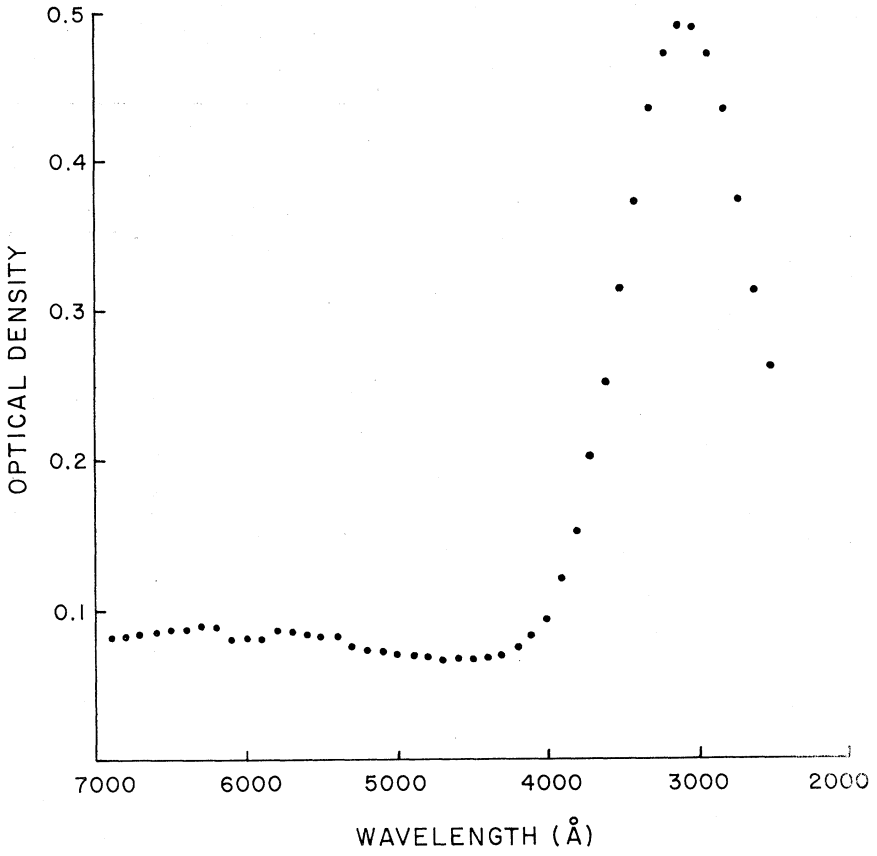

FIG. 7. Optical absorption induced in NH_4HF_2 by electron irradiation. Both the irradiation and the observations were made at approximately 77°K. The major absorption is attributed to F_2^- ions.

electron. The $^2\Sigma_u^+$ to $^2\Sigma_g^+$ hole transition is the strongly allowed σ-polarized transition corresponding to the 348-mμ band. For transitions to π states, only the $^2\Sigma_u^+ \rightarrow {}^2\pi_g$ transition is allowed for π-polarized light and it is weak; it corresponds to the 750-mμ band.

Further correlation of the 306-mμ band in NH_4HF_2 with F_2^- defects was made using polarized light. It was assumed that the absorption resulted from a $^2\Sigma_u^+ \rightarrow {}^2\Sigma_g^+$ transition caused by σ-polarized light. The experimental results are given in Fig. 8 which shows that the polarization $E\|a_0$ gave a much larger absorption than $E\|c_0$. For $E\|a_0$, the electric vector is parallel to the σ bond of the untilted F_2^- ions and perpendicular to the σ bond of the tilted ions. For $E\|c_0$ the electric vector is perpendicular to the untilted F_2^- ions and is almost perpendicular to the tilted F_2^- ions. The σ-bond directions obtained from the ESR data were used to predict the relative intensities for these two polarizations. The ratio predicted is approximately 4 to 1 compared to the observed ratio of about 3 to 1; the difference is thought to result from experimental limitations. Hence this experiment furnishes evidence that the symmetry axis of an F_2^- center is parallel to the polarization direction for major optical absorption and that the optical band and ESR absorption result from the same defect.

V. DISCUSSION

A. Defect Models

Two types of defects which appear to require particle bombardment for their production are found in electron-irradiated NH_4HF_2. These have been described as F_2^- molecular ions in anion sites and as neutral hydrogen atoms in undetermined locations. In $NaHF_2$ only the F_2^- ion is observed. There are good justifications for the F_2^- assignment in NH_4HF_2 and $NaHF_2$.

Important considerations are the number of resonance lines associated with a given defect and the symmetries indicated by the ESR spectra. The ground state of the F_2^- ion has been reported as $\sigma_g^2\pi_u^4\pi_g^4\sigma_u^1(^2\Sigma_u)$ with the hole occupying the antibonding orbital σ_u.[8] Thus the paramagnetic behavior expected for F_2^- would be that of a spin-$\frac{1}{2}$ defect interacting with two fluorine nuclei of spin $\frac{1}{2}$. This would yield for each inequivalent anion site a four-line ESR spectrum as is observed. The four nuclear spin states may be described by $|IM_1\rangle = |11\rangle$, $|10\rangle$, $|1-1\rangle$, and $|00\rangle$. The spectrum would be expected to exhibit a highly anisotropic hyperfine structure with maximum splitting when the dc magnetic field is parallel to the σ bond, or, parallel to the F–F bond direction. This is experimentally observed. The molecular axis of the F_2^- ion corresponds exactly to the normal

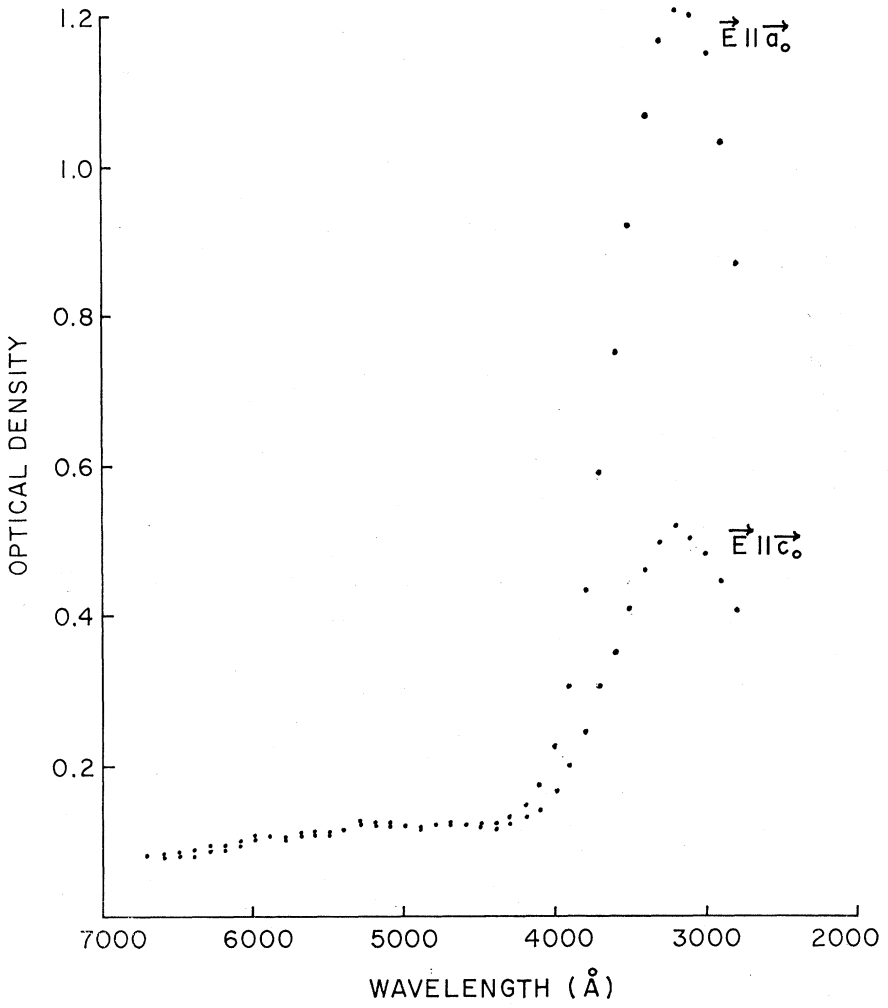

FIG. 8. Dichroic character of the prominent optical-absorption band in electron-irradiated NH_4HF_2 at approximately 77°K. These data give a correlation of the optical and spin resonance centers, which confirms that they each have the same major symmetry axes. The centers are attributed to F_2^- ions in anion sites.

bifluoride axis for F_2^- defects in $NaHF_2$ and also for the untilted $S(1)$ sites in NH_4HF_2; however, for defects in tilted $S(2)$ sites, the axis of an F_2^- ion differs by 8° from that of the related $(FHF)^-$ ion. In $S(2)$ sites, the F_2^- molecular axes lie 8° closer to the a_0b_0 plane. This variation in axis orientation can be explained as resulting from a weakening of the hydrogen bonding between fluorine and nitrogen atoms. The fluorine-fluorine distance in a free F_2^- ion has been calculated[11] as 1.9 Å. Assume this value for an F_2^- defect in the NH_4HF_2; it is much less than the fluorine-fluorine distance of 2.27 Å for a bifluoride ion in NH_4HF_2. Thus, for the defect compared to the anion, the distance between the fluorine and the nitrogen atoms to which they are hydrogen-bonded is lengthened and the hydrogen bond is weakened. This relaxes the tilt angle for a defect in an $S(2)$ site by 8°.

Both the ESR and optical spectra are similar to those reported for F_2^- ions in various materials. Table II[12–14] indicates the similarity of the spin-Hamiltonian parameters for F_2^- ions in a number of fluoride and bifluoride crystals. For all of the examples, a highly anisotropic A tensor is reported with comparable values for the larger component A_z; also all of these defect species exhibit g tensors of similar character with the trace greater than the free-electron g value. The g and A tensors for some of the species appear axial while for others there is evidence of a small amount of rhombic symmetry. Table III gives a comparison of the wavelength for the peak of the major optical absorption by F_2^- ions in different crystals. For different bifluoride crystals this peak does not shift much, whereas the peak is at longer wavelengths for lithium fluoride and for the alkaline earth

[11] T. L. Gilbert and A. C. Wahl, in *Compendium of Ab Initio Calculations of Molecular Energies and Properties*, National Bureau of Standards Technical Note No. 438, edited by M. Krauss (U. S. Government Printing Office, Washington, D. C., 1967), pp. 77, 112.

[12] T. G. Castner and W. Kanzig, J. Phys. Chem. Solids **3**, 178 (1957).

[13] W. Kanzig and T. O. Woodruff, J. Phys. Chem. Solids **9**, 70 (1958).

[14] W. Hayes and J. W. Twidell, Proc. Phys. Soc. (London) **79**, 1295 (1962).

TABLE II. Comparison of spin-Hamiltonian parameters for the F_2^- molecular ion.

Crystal	g_z	g_x	g_y	A_z (in G)	A_x (in G)	A_y (in G)	Reference
KHF_2	2.0020	2.0168	2.0168	955.4	21	21.4	1
(77°K)	±0.001	±0.001	±0.001	±1	±4	±4	
KHF_2	2.0024	2.0180	2.0180	928	35.5	25.5	1
(300°K)	±0.001	±0.0015	±0.0015	±1	±1	±3	
V_k center	2.0031	2.0234	2.0227	887	59	59	12
in LiF	±0.001	±0.001	±0.001				
H center	2.001	2.014	2.012	956	0	0	13
in LiF	±0.002	±0.002	±0.002				
Self-trapped	2.001	2.020	2.020	889.9	48.5	48.5	14
hole in CaF_2	±0.001	±0.001	±0.001		±2	±2	
NH_4HF_2	1.9998	2.0152	2.0152	948.1	15.9	20.6	this paper
(77°K)	±0.0003	±0.001	±0.001	±0.3	±0.1	±0.1	
$NaHF_2$	2.0001	2.0158	2.0158	984.6	64.0	64.0	this paper
(77°K)	±0.0003	±0.001	±0.001	±0.3	±0.1	±0.1	

fluorides. Included in Table III are the approximate temperatures at which the optical absorptions were measured; also included are the original fluorine-fluorine spacings for bifluoride anions in unirradiated bifluoride crystals or for adjacent fluorines in the unirradiated fluorides. Except for the LiF data there appears to be a correlation between the positions of the absorption peak and these fluorine-fluorine spacings, with an increase in wavelength for an increase in spacing. This was reported by Merz and Pershan[15] for certain of these crystals and for other alkali halides. In NH_4HF_2 the optical absorption exhibited strong dichroism with the maximum absorption occurring for the electric vector of the incident light parallel to the F_2^- ion's principal symmetry axis determined by ESR. This strong dichroic behavior is like that reported earlier for the V_K center in LiF.[8]

From momentum transfer considerations, the most likely atomic displacement by electron bombardment is hydrogen. Such a displacement would be required for the generation of the F_2^- ion in the bifluoride crystals. Trapped hydrogen atoms have been observed in NH_4HF_2 following electron irradiation at 77°K which further substantiates the F_2^- identification. The H^0 is readily identified by its isotropic g value near that of the free electron and by its isotropic two-line hyperfine structure. The measured hyperfine splitting of 513±9 G compares closely with that tabulated for H^0 trapped in other matrices.[15] Since the H^0 is not observed in KHF_2 or in $NaHF_2$, one might conclude that the spin resonances are so broad that they escape detection or that the displaced hydrogen atoms are changed into some diamagnetic form, such as protons or hydrogen molecules.

TABLE III. Position of F_2^- optical absorption for several different crystals.

Crystal	Fluorine-fluorine spacing[a] (Å)	Absorption peak (mμ)	Approximate temperature (°K)	Reference
KHF_2	2.26	302	<273°	1
NH_4HF_2	2.27	306	77°	this paper
$NaHF_2$	2.48	308	77°	this paper
		305[b]		
CaF_2	2.73	310	77°	14, 15
		315		
LiF	2.83	348	77°	8
SrF_2	2.93	325	77°	14
BaF_2	3.09	345	77°	14

[a] Fluorine-fluorine spacing corresponds to that between fluorines in normal bifluoride ions for bifluoride crystals or between normal anion positions for the fluoride crystals.
[b] The 305-mμ wavelength was measured after partial annealing which enhanced the resolution and uncovered an absorption band at 230 mμ of different origin.

[15] J. L. Merz and P. S. Pershan, Phys. Rev. 162, 217 (1967).

B. Annealing Behavior

The annealing behaviors of F_2^- ions in NH_4HF_2 and in $NaHF_2$ can be classified as corresponding to second-order kinetics. Detailed models for the annealing processes have not been deduced. One major reason is the difficulty in accounting for the displaced hydrogen atoms since they have been detected only in NH_4HF_2. Even in this material the H^0 resonances are broad and the signal-to-noise ratio prevents good quantitative annealing experiments. For a simple possible model for F_2^- decay in the NH_4HF_2 assume that equal concentrations of F_2^- ions and H^0 atoms exist following the electron bombardment at 77°K. During a pulse anneal the H^0's are readily released from their traps and "look for" F_2^- ions for recombination. Further, assume that the rate constants for other processes which eliminate H^0's are small compared to the rate constant for recombination. Then the hydrogen atom concentration $[H^0]$ would equal the F_2^- concentration $[F_2^-]$ and the rate equation would become

$$\frac{d[F_2^-]}{dt} = -K[F_2^-]^2,$$

which describes a second-order process with K as the rate constant. Thus a simple model and second-order kinetic behavior suggest a recombination mechanism. However, it is likely that models of greater complexity must be tested for a satisfactory explanation of the annealing processes.

ACKNOWLEDGMENTS

The authors are indebted to Dr. F. B. Otto for helpful discussions on the computer analysis and to Dr. L. D. Bogan for his assistance in obtaining the optical data. The computers employed for this work were supplied by the University of Connecticut Computer Center, which is supported in part by Grant No. GP-1819 of the National Science Foundation.

PHYSICAL REVIEW B VOLUME 1, NUMBER 5 1 MARCH 1970

Nuclear Quadrupole Coupling in the LiH Molecule*

CHUN-CHIAN LU† AND R. D. PRESENT
Department of Physics, University of Tennessee, Knoxville, Tennessee 37916
(Received 6 October 1969)

A valence-bond configuration-interaction Slater-orbital wave function for LiH was constructed with all orbital exponents optimized. The orbitals used were Li $1s$, $2s$, $2p\sigma$, $3d\sigma$, and H $1s$, $2p\sigma$; and six configurations were included, all with undeformed inner shells ($1s^2$). The core deformation and the related correction to the nuclear quadrupole coupling constant were then calculated by the method of Sternheimer and Foley, i.e., by first determining the quadrupolarization of the $1s$ shell by the nuclear moment Q and then calculating the interaction of the external molecular charges with the nuclear Q shielded by the quadrupole moment induced in the $1s$ shell. Denoting by q_0 the value of the electric field gradient at the Li nucleus obtained from a wave function with no provision for core deformation and denoting by Δq the correction to q_0 associated with the quadrupolarization of the core, we investigated the sensitivity of q_0 and of $\Delta q/q_0$ to changes in the wave function produced by varying the configuration mixture and altering the values of the orbital exponents. Although q_0 was found to be sensitive to these changes, the fractional Sternheimer correction, $\Delta q/q_0$, was insensitive and in all cases stayed between the limits of -0.22 and -0.24. The final values obtained for q_0 and q are not highly accurate, because of the obvious limitations of the wave function, but the result that $\Delta q/q_0=-0.23$ is reliable enough to be useful in estimating Sternheimer corrections to the results of other workers who have used more elaborate wave functions. Combining the results of several calculations with implicit and explicit Sternheimer corrections, we estimate that $q/2e=(-0.0170\pm0.0013)a_0^{-3}$ and that $Q(\mathrm{Li}^7)=(-4.3\pm0.3)\times10^{-26}$ cm^2.

INTRODUCTION

An accurate value of the electric field gradient q at the Li nucleus of the LiH molecule is needed in order to obtain the electric quadrupole moment Q of the Li^7 nucleus from measurements[1] of the nuclear quadrupole coupling constant (eqQ). As pointed out by Sternheimer and Foley,[2] it is important in calculating q to take account of the deformation of the $1s$ shell surrounding the nucleus by the external electric charges of the molecule. In the following we denote by q_0 the value of q calculated with a molecular wave function that permits no deformation of the spherically symmetric $1s$ shell and we denote the corresponding Sternheimer correction to q for externally induced core deformation by Δq. The separation of q into the two parts, q_0 and Δq, does not occur when the wave function is sufficiently flexible to allow for the distortion of the $1s$ shell and the Sternheimer correction is then not explicit. Four of the previous calculations[3–6] of q in LiH have been made with wave functions that either admixed $3d\sigma$ to $1s$ Slater orbitals or represented the $1s$ orbitals in terms of elliptic coordinates; thus, the Sternheimer effect was implicitly taken into account. While the approximate agreement of the results of these calculations, which were made with different types of wave function, lends confidence to the values of q obtained, it is not certain that the core deformation is adequately taken into account in this way. The variational method deforms the core to produce a charge distribution consistent with the lowest energy but, with an incomplete set of basis functions, there is no assurance that the deformation is realistic and the value of q accurate. Indeed, as the set of basis functions is extended and the energy improved, the value of q could become worse.[7]

An alternate method of treating the problem, proposed by Sternheimer[2] and applied by Sternheimer and Foley[8] to the case of Li_2, employs a wave function which takes no account of core deformation and which gives the value q_0 for the field gradient. It is then shown from perturbation theory[8–10] that the correction $eQ\Delta q$ to the nuclear quadrupole coupling constant can be calculated simply with this wave function by first determining the

* Supported by a grant from the National Science Foundation.
† Present address: Oak Ridge National Laboratory.
[1] L. Wharton, L. P. Gold, and W. Klemperer, J. Chem. Phys. **37**, 2149 (1962).
[2] R. M. Sternheimer, Phys. Rev. **80**, 102 (1950); **84**, 244 (1951); R. M. Sternheimer and H. M. Foley, *ibid.* **92**, 1460 (1953).
[3] S. L. Kahalas and R. K. Nesbet, J. Chem. Phys. **39**, 529 (1963).
[4] J. C. Browne and F. A. Matsen, Phys. Rev. **135**, A1227 (1964).
[5] C. F. Bender and E. R. Davidson, J. Phys. Chem. **70**, 2675 (1966).
[6] C. F. Bender and E. R. Davidson, Phys. Rev. **183**, 23 (1969).
[7] Comparing the results of Refs. 3–5, we note that the calculation which gives the best energy yields the poorest dipole moment and vice versa.
[8] R. M. Sternheimer and H. M. Foley, Phys. Rev. **92**, 1460 (1953).
[9] T. P. Das and R. Bersohn, Phys. Rev. **102**, 733 (1956).
[10] A. Dalgarno, Advan. Phys. **11**, 281 (1962).